Identifying $(BN)_2$-Pyrenes as a New Class of Singlet Fission Chromophores: Significance of Azaborine Substitution

Tao Zeng,*[,†,1] Soren K. Mellerup,[‡,a] Dengtao Yang,[‡] Xiang Wang,[‡] Suning Wang,[‡] and Kevin Stamplecoskie*[‡]

[†]Department of Chemistry, Carleton University, Ottawa, Ontario K1S5B6, Canada

[‡]Department of Chemistry, Queen's University, Kingston, Ontario K7L3N6, Canada

[1] These two authors make equal contributions.

ABSTRACT: Singlet fission converts one photoexcited singlet state to two triplet excited states and raises photoelectric conversion efficiency in photovoltaic devices. However, only a handful of chromophores have been known to undergo this process, which greatly limits the application of singlet fission in photovoltaics. We hereby identify a recently synthesized diazadiborine-pyrene ($(BN)_2$-pyrene) as a singlet fission chromophore. Theoretical calculations indicate that it satisfies the thermodynamics criteria for singlet fission. More importantly, the calculations provide a physical chemistry insight into how the BN substitution makes this happen. Both calculation and transient absorption spectroscopy experiment indicate that the chromophore has a better absorption than pentacene. The convenient synthesis pathway of the $(BN)_2$-pyrene suggests an *in situ* chromophore generation in photovoltaic devices. Two more $(BN)_2$-pyrene isomers are proposed as singlet fission chromophores. This study sets a step forward in the cross-link of singlet fission and azaborine chemistry.

Graphical TOC Entry

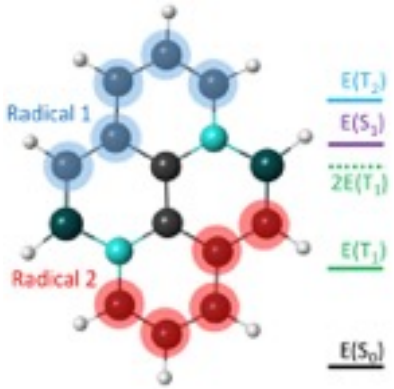

Keywords

Singlet Fission; Azaborine Chemistry; Transient Absorption Spectroscopy; Multireference Perturbation Theory; Small Chromophore

Singlet fission (SF) is a photophysical process that fissions one singlet exciton, generated by absorbing one photon, into two triplet excitons.[2,3] With the doubled number and the longer lifetime of triplet excitons, SF provides an avenue to enhance the maximum photoelectric conversion efficiency for single-junction devices from the ~30% Shockley-Queisser limit to ~45%.[4] The promising application of this phenomenon in organic photovoltaics (OPV) rekindled extensive research interest in this subject in the past decade.[5-6] In a simplified description, SF occurs within two adjacent chromophores:

where (and) stands for the singlet ground state (the lowest singlet and triplet excited states). is a pair of triplet states that are coupled to form an overall singlet. Its generation is an internal conversion process, with a time scale as short as sub-ps.[4,5] In the second step, is decoupled by weak spin-dependent interactions to independent triplets (), with a

---

[2] Smith, M. B.; Michl, J. Singlet fission. *Chem. Rev.* **2010**, *110*, 6891-6936.

[3] Smith, M. B.; Michl, J. Recent Advances in Singlet fission. *Annu. Rev. Phys. Chem.* **2013**, *64*, 361-386.

[4] Hanna, M. C.; Nozik, A. J. Solar conversion efficiency of photovoltaic and photoelectrolysis cells with carrier multiplication absorbers. *J. Appl. Phys.* **2006**, *100*, 074510.

[5] Chan, W.-L.; Ligges, M.; Jailaubekov, A.; Kaake, L.; Miaja-Avila, L.; Zhu, X.-Y. Observing the multiexciton state in singlet fission and ensuing ultrafast multielectron transfer. *Science* **2011**, *334*, 1541-1545.

[6] Xia, J.; Sanders, S. N.; Cheng, W.; Low, J. Z.; Liu, J.; Campos, L. M.; Sun, T. Singlet fission: progress and prospects in solar cells. *Adv. Mater.* **2017**, *29*, 1601652.

~s time scale.[7,8] In solids or oligomers of chromophores, the photogenerated singlet exciton can be delocalized over several chromophores[9,10] and the triplet-pair can migrate apart before losing their spin coupling.[11]

To have thermodynamically favorable SF, chromophores should satisfy the exoergicity conditions:

Equation 1

Equation 2

---

[7] Yayebjee, M. J. Y.; Sanders, S. N.; Kumarasamy, E.; Campos, L. M.; Sfeir, M. Y.; McCamey, D. R. Quintet multiexciton dynamics in singlet fission. *Nature Phys.* **2017**, *13*, 182-188.

[8] Basel, B. S.; Zirzlmeier, J.; Hetzer, C.; Phelan, B. T.; Krzyaniak, M. D.; Reddy, S. R.; Coto, P. B.; Horwitz, N. E.; Young, R. M.; White, F. J.; Hampel, F.; Clark, T.; Thoss, M.; Tykwinski, R. R.; Wasielewski, M. R.; Guldi, D. M. Unified model for singlet fission within a non-conjugated covalent pentacene dimer. *Nature Comm.* **2017**, *8*, 15171.

[9] Casanova, D. Electronic structure study of singlet fission in tetracene derivatives. *J. Chem. Theory Comput.* **10**, 324-334 (2014).

[10] Pensack, R. D.; Tilley, A. J.; Parkin, S. R.; Lee, T. S.; Payne, M. M.; Gao, D.; Jahnke, A. A.; Oblinsky, D. G.; Li, P.-F.; Anthony, J. E.; Seferos, D. S.; Scholes, G. D. Exciton delocalization drives rapid singlet fission in nanoparticles of acene derivatives. *J. Am. Chem. Soc.* **2015**, *137*, 6790-6803.

[11] Scholes, G. D. Correlated pair states formed by singlet fission and exciton-exciton annihilation. *J. Phys. Chem. A* **2015**, *119*, 12699-12705.

which drive the -to-2 fission and prevent the reverse 2-to-, -, and - fusions.[12-13] Furthermore, the inequality makes the -to- intersystem crossing (ISC) thermodynamically unfavorable. The ISC is followed by the efficient -to- decay (Kasha's rule[14]) and results in one exciton. It is detrimental for SF. However, and usually involve - excitations and according to El-Sayed's rule,[15] ISC between them is slow. Therefore, is a weaker requirement than . Due to the rapidity of geometry relaxation, all energies in the two equations are of optimized structures of the corresponding states and ideally include zero point energy (ZPE) corrections. Since the lowest quintet state of a chromophore molecule usually has higher energy than and , Eq. 2 can be omitted. Eq. 1 is the only thermodynamic criterion for SF chromophores to meet. Unfortunately, only a handful of molecules are known to satisfy the inequalities. They include tetracene,[5] pentacene,[4,16]

---

[12] Paci, I.; Johnson, J. C.; Chen, X. D.; Rana, G.; Popović, D.; David, D. E.; Nozik, A. J.; Ratner, M. A.; Michl, J. Singlet fission for dye-sensitizerd solar cells: can a suitable sensitizer be found? *J. Am. Chem. Soc.* **2006**, *128*, 16546-16553.

[13] Casanova, D. Theoretical modeling of singlet fission. *Chem. Rev.* **2018**, DOI: 10.1021/acs.chemrev.7b00601.

[14] Kasha, M. Characterization of Electronic Transitions in Complex Molecules. *Discuss Faraday Soc.* **1950**, *9*, 14-19.

[15] Lower, S. K.; El-Sayed, M. A. The triplet state and molecular electronic processes in organic molecules. *Chem. Rev.* **1966**, *66*, 199-241.

[16] Zeng, T.; Hoffmann, R.; Ananth, N. The low-lying electronic states of pentacene and their roles in singlet fission. *J. Am. Chem. Soc.* **2014**, *136*, 5755-5764.

some of their derivatives,[6,16,17-18] perylenediimide,[19,20] and some polyenes.[21-22] Currently, SF research has been "overwhelmingly limited" to tetracene and pentacene.[12] This limited arsenal of chromophores greatly hinders the advancement of SF research and motivates us to seek new and alternative chromophores that satisfy the criterion.

A series of theoretical studies have clarified that only molecules with non-negligible diradical character and negligible tetraradical character satisfy the inequalities.[23-24] Tuning diradical character is hence a viable way to design new, non-

---

[17] Margulies, E. A.; Wu, Y.-L.; Gawel, P.; Miller, S. A.; Shoer, L. E.; Schaller, R. D.; Diederich, F.; Wasielewski, M. R. Sub-picosecond singlet exciton fission in cyano-substituted diaryltetracenes. *Angew. Chem. Int. Ed.* **2015**, *54*, 8679-8683.

[18] Fuemmeler, E. G.; Sanders, S. N.; Pun, A. B.; Kumarasamy, E.; Zeng, T.; Miyata, K.; Steigerwald, M. L.; Zhu, X.-Y.; Sfeir, M. Y.; Campos, L. M.; Ananth, N. A direct mechanism of ultrafast intramolecular singlet fission in pentacene dimers. *ACS Cent. Sci.* **2016**, *2*, 316-324.

[19] Eaton, S. W.; Shoer, L. E.; Karlen, S. D.; Dyar, S. M.; Margulies, E. A.; Veldkamp, B. S.; Ramanan, C.; Hartzler, D. A.; Savikhin, S.; Marks, T. J.; Wasielewski, M. R. Singlet exciton fission in polycrystalline thin films of a slip-stacked perylenediimide. *J. Am. Chem. Soc.* **2013**, *135*, 14701-14712.

[20] Margulies, E. A.; Miller, C. E.; Wu, Y.; Ma, L.; Schatz, G. C.; Young, R. M.; Wasielewski, M. R. Enabling singlet fission by controlling intramolecular charge transfer in -stacked covalent terrylenediimide dimers. *Nature Chem.* **2016**, *8*, 1120-1125.

[21] Wang, C.; Tauber, M. J. High-yield singlet fission in a zeaxanthin aggregate observed by picosecond resonance raman spectroscopy. *J. Am. Chem. Soc.* **2010**, *132*, 13988-13991.

[22] Musser, A. J; Maiuri, M.; Brida, D.; Cerullo, G.; Friend, R. H.; Clark, J. The nature of singlet exciton fission in carotenoid aggregates. *J. Am. Chem. Soc.* **2015**, *137*, 5130-5139.

[23] Minami, T.; Nakano, M. Diradical character view of singlet fission. *J. Phys. Chem. Lett.* **2012**, *3*, 145-150.

[24] Ito, S.; Nagami, T.; Nakano, M. Molecular design for efficient singlet fission. *J. Photochem. Photobio. C* **2018**, *34*, 85-120.

acene-based SF chromophores. 1,3-diphenylisobenzofuran was the first successfully designed chromophore following this strategy and it does exhibit SF behavior.[25-26] Another emerging class of SF chromophores, non-polycyclic thienoquinoid compounds, were also proposed based on this idea.[27] Small chromophores are especially attractive for OPV application because of the potentially high exciton density that they bring. In the past five years, several small chromophores with about 10 nonhydrogen atoms were proposed based on theoretical studies.[28-29] However, their existence remains only on paper. Here we identify a recently synthesized diazadiborine-pyrene (**1**, see Figure 1(a)) as a promising small SF chromophore.[30]

The development of new synthetic techniques for preparing BN-doped polycyclic aromatic hydrocarbons (PAH) and significant improvements observed for their resulting optoelectronic properties have made azaborine chemistry a thriving field over the past

---

[25] Schwerin, A. F.; Johnson, J. C.; Smith, M. B.; Preearunothai, P.; Popović, D.; Černý, J.; Havlas, Z.; Paci, I.; Akdag, A.; Macleod, M. K.; Chen, X.; David, D. E.; Ratner, M. A.; Miller, J. R.; Nozik, A. J.; Michl, J. Toward Designed Singlet Fission: Electronic States and Photophysics of 1,3-Diphenylisobenzofuran. *J. Phys. Chem. A* **2010**, *114*, 1457-1473.

[26] Johnson, J. C.; Michl, J. 1,3-Diphenylisobenzofuran: a model chromophore for singlet fission. *Top. Curr. Chem.* **2017**, *375*, 80.

[27] Kawata, S.; Pu, Y.-J.; Saito, A.; Kurashige, Y.; Beppu, T.; Katagiri, H.; Hada, M.; Kido, J. Organic photovoltaics: singlet fission of non-polycyclic aromatic molecules in organic photovoltaics. *Adv. Mater.* **2016**, *28*, 1585-1590.

[28] Akdag, A.; Havlas, Z; Michl, J. Search for a small chromophore with efficient singlet fission: biradicaloid heterocycles. *J. Am. Chem. Soc.* **2012**, *134*, 14624-14631.

[29] Bhattacharyya, K.; Pratik, S. M.; Datta, A. Small organic molecules for efficient singlet fission: role of silicon substitution. *J. Phys. Chem. C* **2015**, *119*, 25696-25702.

[30] Wang, S.; Yang, D.-T.; Lu, J.; Shimogawa, H.; Gong, S.; Wang, X.; Mellerup, S. K.; Wakamiya, A.; Chang, Y.-L.; Yang, C.; Lu, Z.-H.; In situ solid-state generation of $(BN)_2$-pyrenes and electroluminescent devices. *Angew. Chem. Int. Ed.* **2015**, *54*, 15074-150784.

two decades.[31-32] Being donor and acceptor, respectively, sp^2 N and B exert the captodative effect to the carbon fragment that they sandwich and stabilize its radical character.[33] Therefore, CC replacement by a BN unit is an efficient way to enhance diradical character of a system, thereby making it satisfy the SF inequalities. Although there have been theoretical studies in designing SF chromophores based on BN embedded conjugated systems,[42,34,35] **1** represents the first synthesized example. Its pyrene core has 16 nonhydrogen atoms, two fewer than tetracene, the smallest known molecule to satisfy the requisite inequalities. Quantum chemistry calculations are performed to show that **1** satisfies the energy inequalities and, more importantly, explain why so. The advantages of using **1** as SF chromophores are discussed. Especially, the large transition dipole moment between the ground and the first excited state is confirmed by transient absorption spectroscopy. In addition to molecule **1**, through quantum chemistry calculations, two previously unknown diazadiborine-pyrenes are proposed as potential SF chromophores.

---

[31] Liu, Z.; Marder, T. B. B-N versus C-C: How similar are they? *Angew. Chem. Int. Ed.* **2008**, *47*, 242-244.

[32] Mellerup, S. K.; Li, C.; Tai, P.; Wang, S. Regioselective photoisomerization/C-C bond formation of asymmetric ppyB(Mes)(Ar): the role of aryl groups on boron. *Angew. Chem. Int. Ed.* **2017**, *56*, 6093-6097.

[33] Viehe, H. G.; Janousek, Z.; Merenyi, R.; Stella, L. The captodative effect. *Acc. Chem. Res.* **1985**, *18*, 148-154.

[34] Zeng, T.; Goel, P. Design of small intramolecular singlet fission chromophores: an azaborine candidate and general small size effects. *J. Phys. Chem. Lett.* **2016**, *7*, 1351-1358.

[35] Zeng, T. Through-linker intramolecular singlet fission: general mechanism and designing small chromophores. *J. Phys. Chem. Lett.* **2016**, *7*, 4405-4412.

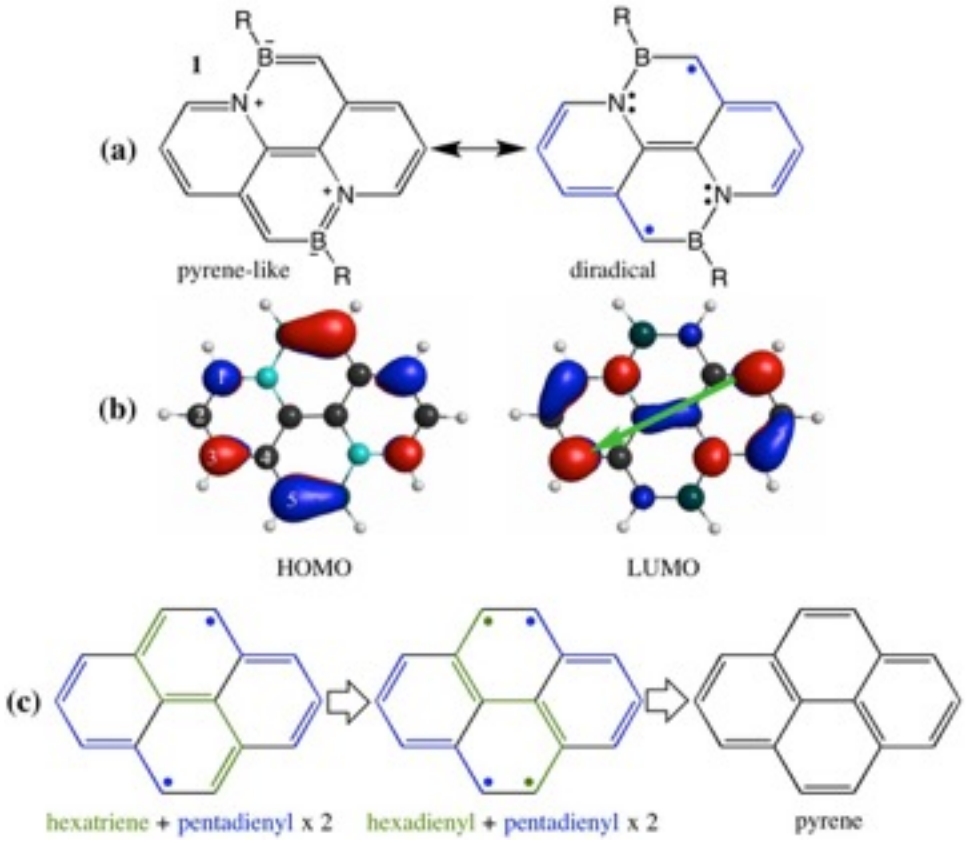

Figure 1. (a) The diazadiborine-substituted pyrene **1** in resonance between a pyrene-like closed-shell and a diradical structure; (b) HOMO and LUMO of **1**; (c) conversion of the diradical structure to closed-shell structure in unsubstituted pyrene. Black, cyan, dark green, and white spheres represent C, N, B, and H atoms. The red and blue lobes represent the opposite phases of the molecular orbitals. The green arrow in the LUMO plotting indicates the direction of the -to- transition dipole moment.

Quantum Chemistry Calculations for 1. Technical details of our Density Functional Theory (DFT) and General Multi-Configurational Quasi-Degenerate Perturbation Theory (GMC-QDPT) calculations are given in the end of this letter. The calculated low-lying excitation energies of **1** (R = H) are summarized in Table 1. They are

obtained by adding (TD)DFT ZPE-corrections to GMC-QDPT excitation energies. Both and are dominated by HOMO-to-LUMO 1-electron excitation. The ZPE-corrected E_{abs}() and E_{fluo}() are 2.24 and 2.13 eV, corresponding to 554 and 582 nm wavelengths. Their excellent agreements with the experimentally observed wavelengths of 562 and 573 nm for **1** (R = mesityl (Mes), in THF) in Ref. 45 corroborate the accuracy of our calculations. Note that we have set R = H in Figure 1 to simplify the calculations, while the experimental wavelengths were obtained for **1** with R = Mes. Time-dependent (TD)DFT calculations show that the R = H by R = Ph replacement results in only a 0.02 eV change in E(). All our reported quantum chemistry results are obtained from gas phase single molecule calculations. A test (TD)DFT calculation for the E_{abs}() using the conductor-like polarizable continuum model[36] to describe the solvent effects of THF shows that the solvent only shifts the energy from the gas phase value by 0.001 eV. The insignificant solvent effects allow us to compare our gas phase GMC-QDPT excitation energies with the experimental values obtained in THF. The ZPE-corrected minimum-to-minimum E_{00}() and E_{00}() are 2.20 and 1.03 eV. They satisfy Eq. 1, with E_{00}() – 2E_{00}() = 0.14 eV. This excess energy is convenient, as it gives some room for bathochromic shifting of E() when **1** is dissolved in solvents, embedded in host materials, or forms a crystal. is dominated by HOMO−1-to-LUMO 1-electron excitation. E_{00}() > E_{00}() by 0.17 eV and satisfies Eq. 1. Given that $(BN)_2$-pyrene **1** satisfies both inequalities in Eq. 1, it can therefore be considered a previously unknown and synthetically viable SF chromophore.

---

[36] Barone, V.; Cossi, M. Quantum calculation of molecular energies and energy gradients in solution by a conductor solvent model. *J. Phys. Chem. A* **1998**, *102*, 1995-2001.

Likewise interesting is the 1.18 eV ZPE-corrected vertical $E()$ calculated at the structure, twice of which is larger than the 2.24 eV $E_{abs}()$ by 0.12 eV. The calculated bond lengths indicate that the -to- and -to- structural reorganizations are in the same direction (see Section S1 in the Supporting Information (SI) for details). For a dimer of **1**, $2E() > E()$ at the vertical structure, $2E() < E()$ at the respective optimized structures of the two states, and the two states relax their structures in the same direction. All these three factors together imply that the potential energy surfaces of the single- and the double-excitonic states cross when the dimer relaxes its structure after photoexcitation (see Figure S2 and the relevant discussion in SI). As demonstrated by Figure 3(A) in Ref. 28 and the relevant discussion therein, such a crossing in the forward region of the reorganization is beneficial for efficient SF.

Table 1. Quantum chemistry calculation results of the promising SF chromophores in this work. All energy quantities are in given eV. All states' energies except $E_{00}()$s are relative to the ground state energy at ground state optimized structure of the respective molecules. $E_{00}()$s are relative to the ground state energy of **1**. Symmetry labels are given beside the structure and energies when needed.

	1, C_{2h}	**1'**, C_{2v}	**2**, C_{2h}	**3**, C_{2h}
n_{LUNO}, n_{LUNO+1}	0.17, 0.07	0.34, 0.11	0.11, 0.09	0.16, 0.09
HOMO-LUMO gap	2.52	2.13	2.94	2.92
$E_{00}()^{\dagger}$	2.20, ^1B_u	2.12, $^1A_1$	2.48, ^1B_u	2.72, ^1B_u
$E_{00}()$	1.03, ^3B_u	0.48, $^3A_1$	1.25, ^3B_u	1.29, ^3B_u

$E_{00}() - 2E_{00}()$	0.14	1.16	–0.02	0.14
$E_{00}()$	2.37, ^3A_g	1.78, $^3B_1$	3.29, ^3A_g	2.83, ^3A_g
$E_{abs}()^{\S}$	2.24	2.20	2.62	2.82
$E_{fluo}()^{\S}$	2.13	2.11	2.43	2.68
$E_{phos}()^{\S}$	0.83	0.42	1.10	1.15
$E_{00}()$ rel. to **1**	0.00	0.29	-1.28	-1.38
d_{01} (a.u.)$^{\#}$	1.97	1.72	1.71	1.89

† The subscript "00" indicates a minimum-to-minimum excitation energy with ZPE corrections of the ground and the excited states. § The subscripts "abs", "fluo", and "phos" indicate vertical absorption, fluorescence emission, and phosphorescence energies calculated at optimized structures of respective initial states, , , and . They all contain ZPE corrections. $^{\#}$ TDDFT calculated transition dipole moment for vertical -to- excitation.

Having identified **1** as a new type of SF chromophore, we turn our attention to understanding why this is the case. In doing so, we can generalize this strategy and propose a family of $(BN)_2$-pyrene SF chromophores, instead of just one. The reason compound **1** satisfies Eq. 1 is clear upon examining the highest occupied and lowest unoccupied molecular orbitals (HOMO and LUMO) plotted in Figure 1(b). The HOMO fragment of the five C atoms (numbered in the figure, termed C1-C5 below) between N and B resembles the nonbonding singly occupied MO (SOMO) of the pentadienyl radical. This fragmental orbital is stabilized through a bonding interaction between C5

and the adjacent B acceptor. Therefore, the HOMO of **1** can be viewed as an antisymmetric combination of two B-stabilized pentadienyl SOMOs. The LUMO fragment of C1-C5 also resembles the pentadienyl SOMO. The minute bonding interaction between C1 and C2 results from the antibonding interaction between C1 and the adjacent N donor, which polarizes the C1 atomic orbital towards C2. Therefore, the LUMO of **1** can be viewed as a symmetric combination of the two N-destabilized pentadienyl SOMOs. The primarily nonbonding character of HOMO and LUMO is consistent with the small structural difference in the and states (≤ 0.02 Å in all bond lengths, see Figure S1 in SI) and the associated small Stoke's shift (0.04 eV from spectra recorded in THF; also see Figure 2(d) below) between the -to- absorption and the -to- fluorescence. There is no substantial gain or loss of bond strength in the transition.

The B-stabilization and N-destabilization opens the HOMO-LUMO gap from 0 of a true diradical with two pentadienyl fragments to 2.52 eV in **1**, compared to the 3.81 eV gap in the unsubstituted pyrene. The smaller HOMO-LUMO gap leads to a larger occupation number in the lowest unoccupied natural orbital (LUNO), n_{LUNO} = 0.17, vs. 0.10 in pryene. Except for molecules with strong ionic character, a small HOMO-LUMO gap correlates with a large n_{LUNO}. The larger n_{LUNO} clearly indicates more significant diradical character in **1** compared to pyrene.[34,35] For all structures discussed in this work, the highest occupied and the lowest unoccupied natural orbital (HONO and LUNO) resemble HOMO and LUMO, respectively. With the significant increase in diradical

character, the diazadiborine substitution has converted pyrene, whose $E_{00}() = 3.37$ eV[37] < $2E_{00}() = 2 \times 2.09$ eV[38], to a molecule that satisfies $E_{00}() > 2E_{00}()$.

The diradical character of **1** is demonstrated by the resonance structure in Figure 1(a), in which the two pentadienyl radical fragments are highlighted in blue. This is a typical case of captodatively enriched diradical character: each pentadienyl radical fragment is sandwiched and stabilized by a B acceptor and a N donor. The idea of using BN substitution to design SF chromophores[42] is realized in **1**. Very importantly, the odd (C1,3,5) positions of the pentadienyl fragments, where the SOMOs are mainly distributed, are not in contact. If the odd positions are in contact, there will be an overlap between the two SOMOs, forming a bonding HOMO and an antibonding LUMO and enlarging the HOMO-LUMO gap. Such a covalent interaction inevitably reduces diradical character and makes a molecule less likely to satisfy Eq. 1. Likewise importantly, the odd positions are not in contact with the central vinyl fragment, otherwise, similar covalent bonds between the radicals and the two central C atoms will occur, resulting in two hexatriene moieties and reducing diradical character.

The significance of the azaborine substitution can also be seen by embedding the dipentadienyl diradical resonance structure in the unsubstituted pyrene. As shown in Figure 1(c), such a resonance structure leaves a hexatriene moiety at the center, which

---

[37] Baba, M.; Saitoh, M.; Kowaka, Y.; Taguma, K.; Yushida, K.; Semba, Y.; Kasahara, S.; Yamanaka, T.; Ohshima, Y.; Hsu, Y.-C.; Lin, S. H. Vibrational and rotational structure and excited-state dynamics of pyrene. *J. Chem. Phys.* **2009**, *131*, 224318.

[38] Avakian, P.; Abramson, E. Singlet-triplet exciton absorption spectra in naphthalene and pyrene crystals. *J. Chem. Phys.* **1965**, *43*, 821-823.

can rearrange to a hexadienyl diradical with two unpaired electrons at the two ends and form π bonds with the unpaired electrons of the pentadienyls. The result is the typical closed-shell structure of pyrene. The rearrangement of the hexatriene moiety is an easy process since no formal charges are needed. The diradical character in pyrene is hence diminished. On the contrary, a similar rearrangement in **1** requires adding formal charges +1 and −1 to N and B, respectively (Figure *1*(a)). Such a counter-electronegativity formal electron transfer from N to B mitigates the dominance of the pyrene-like closed-shell structure and enhances the diradical character in **1**.

Potential advantages of utilizing 1 as a SF chromophore. Compared to the most intensely investigated chromophore pentacene,[1,2] which is the "champion" of SF,[39] **1** features the following advantages. **1** was first synthesized as an effective fluorophore and features a large -to- transition dipole moment (d_{01}). The TDDFT calculated d_{01} magnitude is 1.97 a.u. (atomic unit), more than twice that calculated at the same level of theory for pentacene (0.92 a.u.). Therefore, the low absorptions problem of acene-based SF chromophores, which limits the efficiency of SF-based solar cells,[40] is alleviated by **1**. The complication of introducing a separate absorber layer and connecting it to the SF sensitizer[41] can be avoided. The larger d_{01} is attributed to the fact that the product of the

---

[39] Buchanan, E. A.; Havlas, Z.; Michl, J. Singlet fission:optimization of chromophore dimer geometry. *Adv. Quantum Chem.* **2017**, *75*, 175-227.

[40] Lee, J.; Jadhav, P.; Reusswig, P. D.; Yost, S. R.; Thompson, N. J.; Congreve, D. N.; Hontz, E.; Van Voorhis, T.; Baldo, M. A. Singlet exciton fission photovoltaics. *Acc. Chem. Res.* **2013**, *46*, 1300-1311.

[41] Reusswig, P. D.; Congreve, D. N.; Thompson, N. J.; Baldo, M. A. Enhanced external quantum efficiency in an organic photovoltaic cell via singlet fission exciton sensitizer. *Appl. Phys. Lett.* **2012**, *101*, 113304.

HOMO and LUMO in Figure 1(b) spans over a distance of approximately two benzene rings (see the green arrow in the figure). In pentacene, the product points along the molecule's short axis and only spans over a distance of one benzene ring (see Figure S3 for comparison).

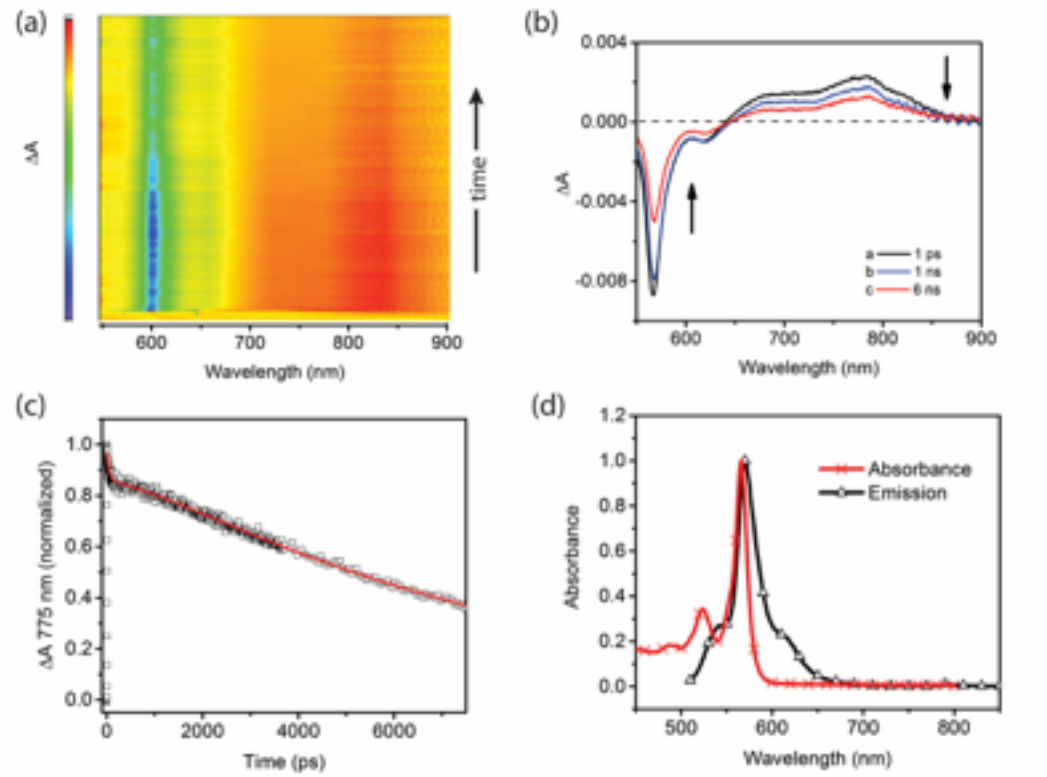

Figure 2. (a) Transient absorption spectrum of **1** in benzene solution, excited with 514 nm femtosecond laser pulse and with measured absorbance over an 8 ns delay time; (b) differential absorption spectra at different times after the pulsed laser excitation; (c) normalized transient absorption profile as a function of time measured at 775 nm; (d) steady-state absorbance and emission spectra of **1** for reference.

The larger d_{01} is corroborated by our femtosecond transient absorption spectroscopy (fsTAS) in Figure 2(a). Using principle component analysis, the spectra can

be well described by a single excited state (i.e.) so that the transient absorption and emission are both a measure of the -to- transition. This is further confirmed in Figure 2(b), where the transient absorption profile maintains the same features immediately after excitation (1 ps) and at longer times (1-6 ns). The kinetics of relaxation of-to- requires multiple components: a 48 ps fast relaxation that we attribute to internal conversion, a 7.76 ns lifetime (for the -to- emission), and a growth (1.3 ± 0.2 ns). The three-component fit is shown in Figure 2(c) and more details of the three components can be found in Section S3 of the SI. The growth of the signal could potentially be explained by the fusion of the bound triplet pair, which is generated by SF. However, without the ability to monitor transient absorption of transparent films, we are unable to make this attribution definitively. The emission occurs at 570 nm in benzene solution, as confirmed by the steady emission spectrum in Figure 2(d), with a quantum yield of 0.59 ± 0.05 (see Experimental Details in the end of the letter). We use the formula to calculate the oscillator strength *f*. In this formula, *n* is the refractive index (0.15 for benzene), the quantum yield (0.59), nm, and = 7.76 ns the lifetime. The meanings of all the other symbols are well known. The *f* is estimated to be 0.11, from which $|d_{01}|$ is estimated to be 1.44 a.u., which is in qualitative agreement with the 1.97 a.u. TDDFT value. There is no doubt that **1** has a larger -to- transition dipole and therefore better absorption than pentacene.

Second, the 1.03 eV E_{00}() of **1** is higher than the 0.86 eV counterpart of pentacene and matches the optimal ~1.0 eV band gap to maximize efficiency of a SF-based solar cell.[1,3] The higher lying state also enlarges the pool of available acceptors that can

harvest the triplet excitons,[62] leads to a slower rate of triplet recombination, and increases open circuit voltage in such devices.[12]

Third, pentacene is well-known to be highly air-sensitive and difficult to work with. In contrast, compound **1** is stable for days in crystalline state under ambient conditions. The stability and the high *E*() of **1** are correlated, as the high *E*() reflects a not too much diradical character. Also, the method by which **1** is prepared facilitates a unique opportunity for its use as a SF chromophore. **1** can be generated *in situ* via elimination reaction of its even more air stable precursor, pre-**1** (Figure 3), either photolytically (PE, driven by solar photons with energy >350 nm) or electrically (exciton-driven elimination, EDE), with the electricity generated by the photovoltaic devices themselves.[45] This concept of *in situ* generation of SF chromophores may provide solutions for the photostability and thin-layer processing problems that plague SF-based OPV devices.

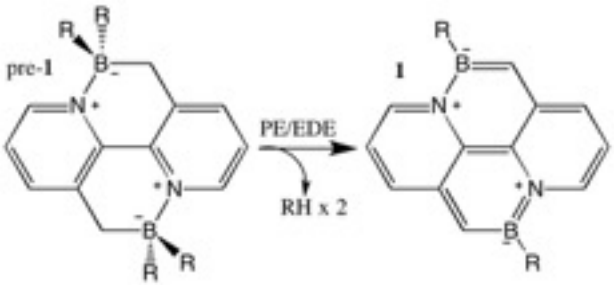

Figure 3. The pre-**1** to **1** conversion through photolytic or exciton-driven elimination.

Fourth, the core structure of **1** has only 16 non-hydrogen atoms, smaller than tetracene. Although the R groups attached to the B atoms increase its size, they can theoretically be replaced by smaller groups. The identification of **1** being a SF chromophore sets a step forward in seeking new, small SF chromophores.

Other proposed $(BN)_2$-pyrene SF chromophores. Inspired by **1**, we performed calculations for ten other $(BN)_2$-pyrenes and investigated their potential of being SF chromophores. Since our synthetic technique is based on photolytic or thermal elimination reactions of benzyl-pyridyl BR_2 chelate compounds to remove one R–H (e.g., Figure 3), we will primarily consider $(BN)_2$-pyrenes with peripheral B atoms that have adjacent $–CH_2$ groups in their pre-elimination forms. Given that molecules bearing two identical BN moieties are more synthetically viable targets, we limit our search to $(BN)_2$-pyrenes with C_{2h} and C_{2v} symmetries. Including **1**, in total eleven C_{2h} and C_{2v} $(BN)_2$-pyrene structures were examined. Throughout this work, numeric indicators with and without prime (') are used to denote C_{2v} and C_{2h} structures, respectively.

1' is the C_{2v} symmetric counterpart of **1**. Its calculated excitation energies are listed in Table 1. $E_{00}() > 2E_{00}()$ is satisfied. **1'** possesses more diradical character than **1**, as reflected by its $n_{LUNO} = 0.34$ (double that of **1**) and low $E_{00}() = 0.48$ eV. Both and arise from HOMO-to-LUMO excitation. The low $E_{00}()$ is far from the optimal ~1 eV band gap, and also implies a waste of energy in SF, *i.e.*, $E_{00}() – 2E_{00}() = 1.16$ eV. The substantial diradical character of **1'** suggests an increased instability; DFT calculations indicate that it is 0.29 eV higher in energy than **1**. The HONO and LUNO in Figure 4(b) point to the diradical resonance structure that contains an allyl and a heptatrienyl radical fragment that are isolated by the two BN units. The two fragments are highlighted in blue in the diradical resonance structure in Figure 4(a). The heptatrienyl is only in contact with the B-acceptors and the allyl only with the N-donors. Consequently, the HOMO of **1'** arises from the allyl SOMO and the B-stabilized heptatrienyl SOMO, while the LUMO

arises from the N-destabilized allyl SOMO and the heptatrienyl SOMO. This is different from **1**, where HOMO (LUMO) has B-stabilization (N-destabilization) for both radical SOMOs. The less stabilized HOMO and less destabilized LUMO leads to a smaller 2.13 eV HOMO-LUMO gap in **1'**, and hence more substantial (too much) diradical character.

Another problem of **1'** is its low E_{00}() (1.78 vs. its 2.12 eV E_{00}()), opening the doorway for the -to- ISC. The low E_{00}() results from the substantial tetraradical character of **1'**, which is reflected by its larger n_{LUNO+1} = 0.11, vs. 0.07 of **1**; n_{LUNO+1} is an indicator of tetraradical character.[34,35] The distributions of the HONO–1 and LUNO+1 amplitudes in Figure 4(b) point to the tetraradical resonance structure in Figure 4(a), which is induced by forming the sextet out of the heptadienyl radical and the central vinyl. E_{00}() is significantly larger than 2E_{00}() by 0.82 eV.

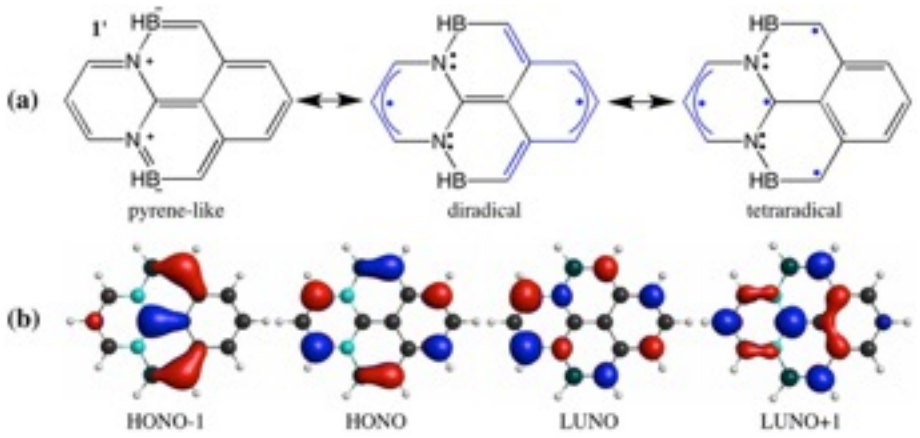

Figure 4. (a) The resonance structures and (b) the frontier natural orbitals of **1'**. Radical fragments in (a) are highlighted in blue.

Structure **2** has E_{00}() = 2.48 eV and E_{00}() = 1.25 eV. The 0.02 eV endoergicity in the SF of **2** is minute. We can view **2** as a chromophore candidate of having isoergic or

slightly endoergic SF. The diradical resonance structure of **2** is shown in the middle of Figure 5(a). It is favored by the formation of the aromatic naphthalene moiety. The large diradical character of the C fragment (not the whole molecule **2**) is reflected by the small E_{00}() of 0.44 eV and n_{LUNO} = 0.28 of the 1,5-naphthoquinodimethane in Figure 5(b); it is a naphthalene analogue of *o*- or *p*-quinodimethane diradicaloid. Please note that *p*-quinodimethane is the fundamental structure, based on which 1,3-diphenylisobenzofuran was designed as a SF chromophore.[37-39] Both the HONO and LUNO in Figure 5(c) have nonbonding amplitudes at the C atoms adjacent to the N atoms, which are consistent with the description of the diradical resonance structure. With an additional competing hexaene closed-shell resonance structure (Figure 5(a)), the diradical resonance form naturally weights less compared to **1**. This is reflected by the smaller n_{LUNO} = 0.11 and the larger HOMO-LUMP gap of 2.94 eV of **2** Less diradical character corresponds to higher E_{00}(), which makes the SF slightly endoergic. E_{00}() > E_{00}() by 0.81 eV in **2**.

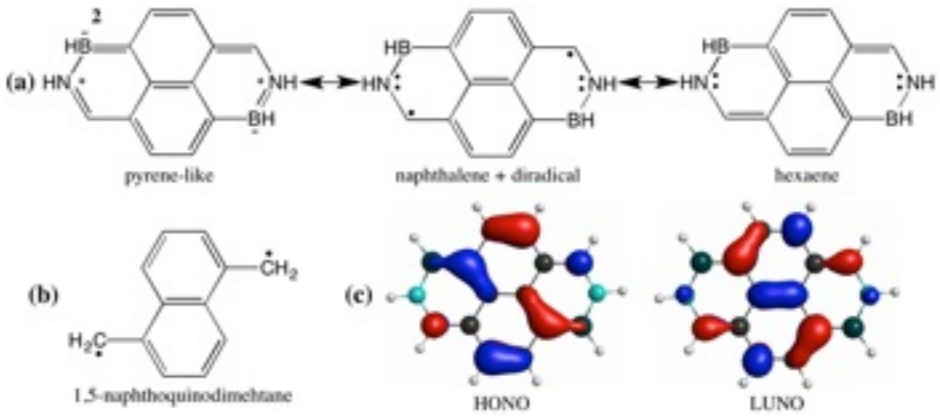

Figure 5. (a) The resonance structures and (b) the HONO and LUNO of **2**.

Structure **3** is similar to **2**, but with the N and B positions being swapped. With an identical C fragment, **3** is expected to share similar resonance structures with **2**, as shown in Figure 6(a). The HONO and LUNO in Figure 6(b) also share similarities with the counterparts in Figure 5(c). A main difference in the orbitals is the significantly larger amplitudes at the two C atoms not within the naphthalene fragment. This suggests a larger diradical character in **3** *vs.* **2**, which is confirmed by the larger n_{LUNO} = 0.16 of **3**. The two radical centers in **3** are adjacent to and stabilized by the B-acceptors, while in **2**, they are adjacent to and destabilized by the N-donors. The larger diradical character makes **3** satisfy $E_{00}(\text{}) = 2.72$ eV > $2E_{00}(\text{}) = 2.58$ eV. $E_{00}(\text{}) > E_{00}(\text{})$ by 0.11 eV in **3**. **3** is a more promising SF chromophore than **2** not just because of its more favorable excitation energies. Our experience in azaborine syntheses suggests that the photolytic elimination of endocyclic -R_2B-CH_2- to -RB=CH- is more convenient than the elimination of endocyclic -R_2B-CHR- to -RB=CR-. With a H on the C atoms adjacent to the B atoms, **3** shall be more synthetically viable than **2**.

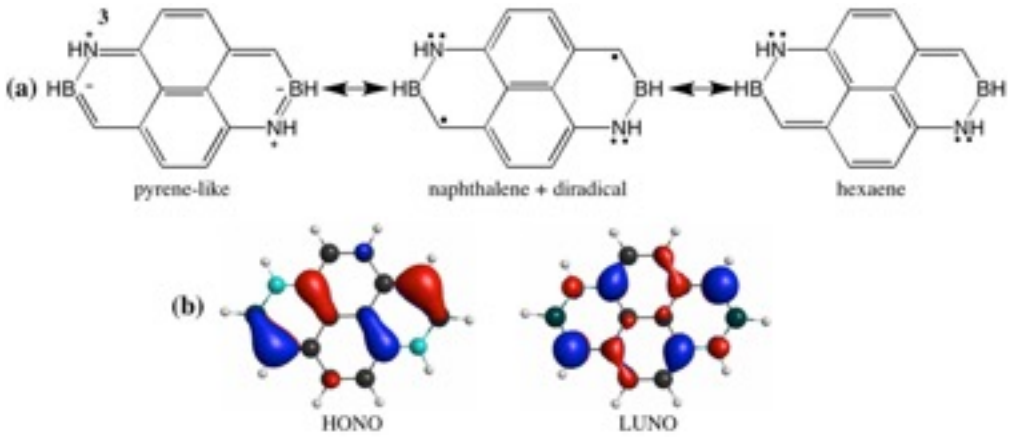

Figure 6. (a) The resonance structures and (b) the HONO and LUNO of **3**.

All three additional $(BN)_2$-pyrenes that satisfy (or nearly satisfy) $E_{00}() > 2E_{00}()$ have been discussed. Their calculated results are summarized in Table 1. They all possess d_{01}s that are about twice as large as that of pentacene. Also included in the table are their DFT ground state energies ($E_{00}()$s) relative to **1**. **2** and **3** are more stable than **1** by > 1 eV, and their $E()$s are high yet not far from the optimal 1 eV. The two molecules, especially **3**, should therefore be considered high value synthesis targets. The BN/CC isosterism and isoelectronicity naturally lead to the dominant pyrene-like resonance structures in the four substituted structures discussed above. These pyrene-like resonance structures, however, all contain formal charges on B and N, which mitigate their dominance. In their uncharged resonance structures, radical fragments can be easily identified, and the associated enhanced diradical characters make the four molecules satisfy the energy criterion. The other seven $(BN)_2$-pyrenes, shown in Figure 7, do not satisfy $E_{00}() > 2E_{00}()$ and are of less interest in the context of SF. Their reasons of not satisfying the inequality are thoroughly discussed in Section S4 of the SI. In short, they lack diradical resonance structures without formal charges on N and B. The most pronounced formally uncharged resonance structures of the seven isomers are shown in Figure 7, with the C fragments highlighted in colors. These resonance structures are inferred from the frontier orbitals of the molecules. None of the C fragments exhibit diradical character, in strong contrast to those shown in Figures 1, 4-6. Evidently, the significance of azaborine substitutions in designing SF chromophores is to isolate C fragments that have clear diradical character in the uncharged resonance structures. In this work, this strategy is applied to the pyrene

pristine structure. It is very natural to apply this strategy to other pristine structures, which broadens the application of azaborine chemistry in photovoltaics research.

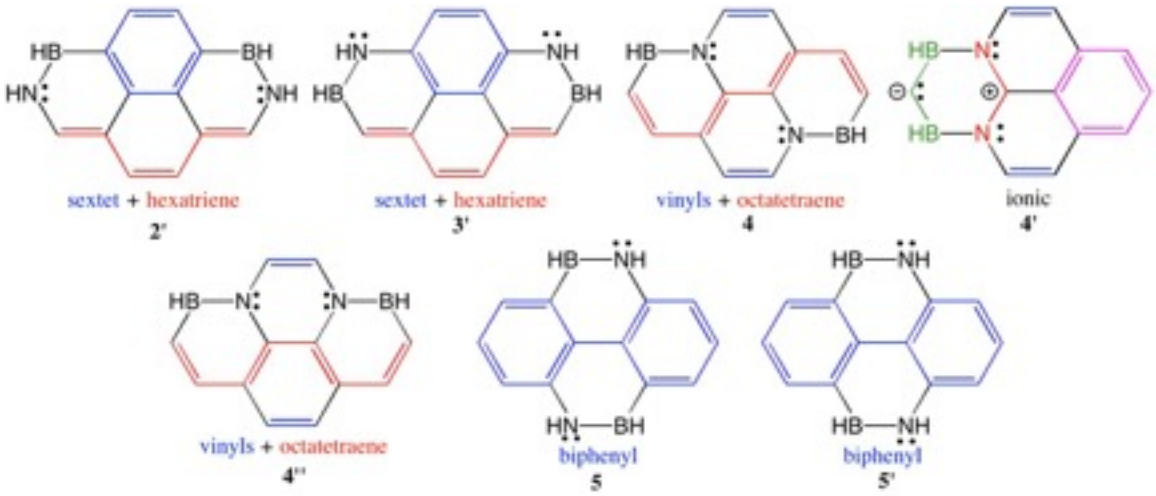

Figure 7. The seven additional $(BN)_2$-pyrene structures that are studied in this work but do not satisfy $E_{00}() > 2E_{00}()$.

In conclusion, we identify a recently synthesized diazadiborine-substituted pyrene (**1**) as a singlet fission chromophore through quantum chemistry calculations. A new optoelectronic function is found for this fluorophore. The $(BN)_2$-pyrene can be viewed as being composed of two captodatively stabilized pentadienyl radicals. The substantial diradical character makes it satisfy the $E() > 2E()$ exoergic criterion for singlet fission. The similar structural reorganizations in and of the $(BN)_2$-pyrene and the change of the $E()$ and $2E()$ relation in the reorganizations indicate a crossing between the single- and multi-excitonic states in the forward region of structural relaxation after excitation. This crossing is known to kinetically facilitate singlet fission. The $(BN)_2$-pyrene features the following potential advantages for being a singlet fission chromophore: large absorption, high triplet energy, high stability, and small size of its core structure. The large transition

dipole moment between the ground and the first singlet excited state of the molecule is confirmed by femtosecond transient absorption spectroscopy. Furthermore, the molecule's synthesis pathway through photolytic or electricity-driven elimination of its highly stable precursor suggests an *in situ* generation of the chromophore in an OPV device. We have also performed calculations for ten other diazadiborine-substituted pyrenes with symmetrically identical BN moieties, which have not been synthesized. Three appear to have enough diradical character to satisfy the exoergic criterion and have large absorptions. Two of them (**2** and **3**) are thermodynamically more stable than **1** and have high triplet energies. They are high value targets for future syntheses. The ultimate goal of this work is to crosslink the two vibrant fields of singlet fission and azaborine chemistry. A step forward in this direction has certainly been made. Azaborine compounds as singlet fission chromophores are no longer just designs on paper.

COMPUTATIONAL DETAILS

All calculations except the hessian calculations are carried out using GAMESS-US[42] with Dunning's cc-pVDZ basis set.[43] The hessian calculations are carried out using

[42] Schmidt, M. W.; Baldridge, K. K.; Boatz, J. A.; Elbert, S. T.; Gordon, M. S.; Jensen, J. H.; Koseki, S.; Matsunaga, N.; Nguyen, K. A.; Su, S.; Windus, T. L.; Dupuis, M.; Montgomery Jr., J. A. General atomic and molecular electronic structure system. *J. Comput. Chem.* **1993**, *14*, 1347-1363.

[43] Dunning, T. H. Gaussian basis sets for use in correlated molecular calculations. I. The atoms boron through neon and hydrogen. *J. Chem. Phys.* **1989**, *90*, 1007-1023.

ORCA[44] with the same basis set. All investigated molecules have their structures optimized at the restricted DFT level, optimized at the unrestricted DFT level, and optimized at the TDDFT level. The B3LYP functional[45,46] is used in all (TD)DFT calculations. Hessian calculations are carried out for all optimized structures to confirm that they are minima on potential energy surfaces and give the ZPE corrections. From the (TD)DFT energies, we identify four structures (**1**, **1'**, **2**, and **3**) that (nearly) satisfy $E() > 2E()$. At their optimized structures, the General Multi-Configurational Quasi-Degenerate Perturbation Theory (GMC-QDPT) calculations[47-48] are performed to re-estimate their excitation energies. The active space of each $(BN)_2$-pyrene includes 10 electrons in 10 orbitals. The highest lying 5 occupied and the lowest lying 5 unoccupied orbitals obtained in ground state DFT calculation are used as initial guess of the active orbitals, which are optimized in the CASSCF calculation in preparing reference states of the GMC-QDPT treatment. As an example of the active spaces, the natural orbitals of the ground state of **1** and their occupation numbers are shown in Figure S12 in SI. The largest

---

[44] Neese, F. The ORCA program system. *Wiley Interdiscip. Rev. Comput. Mol. Sci.* **2012**, *2*, 73-78.

[45] Becke, A. D. Density-functional thermochemistry. I. The effect of the exchange-only gradient correction. *J. Chem. Phys.* **1992**, *96*, 2155-2160.

[46] Lee, C.; Yang, W.; Par, R. G. Development of the Colle-Salvetti correlation-energy formula into a functional of the electron density. *Phys. Rev. B* **1988**, *37*, 785-789.

[47] Nakano, H.; Uchiyama, R.; Hirao, K. Quasi-degenerate perturbation theory with general multiconfiguration self-consistent field reference functions. *J. Comput. Chem.* **2002**, *23*, 1166-1175.

[48] R. Ebisuzaki; Y. Watanabe; Nakano, H. Efficient implementation of relativistic and non-relativistic quasidegenerate perturbation theory with general multiconfigurational reference functions. *Chem. Phys. Lett.* **2007**, *442*, 164-169.

and the smallest occupation numbers of these orbitals are close to 2 and 0, respectively, indicating the adequacy of the active space. All GMC-QDPT excitation energies are obtained in a state-averaged manner. All discussed HOMOs and LUMOs and their gaps are obtained from ground state DFT calculations, while the natural orbitals and their occupation numbers are obtained from ground state GMC-QDPT calculations.

EXPERIMENTAL DETAILS

$(BN)_2$-pyrene **1** was prepared according to a known procedure.[45] Quantum yield of fluorescence was measured using a Hamamatsu absolute QY spectrometer (C11347-11). Previously,[45] the QY of **1** was measured to be 27% in THF according to the optically dilute method while employing $Ir(ppy)_3$ as the standard. Utilizing a Hamamatsu spectrometer, this value increases to 40.5% ± 5% in THF and 59.1% ± 5% in C_6H_6. Given that the absorption and emission of $Ir(ppy)_3$ do not match those of BN-pyrene **1**, it is expected that the QY measured according to the optically dilute method is inaccurate. We therefore take the values obtained by the absolute spectrometer to be correct.

Ultrafast pump/probe spectroscopy (fsTAS) measurements were performed on an Ultrafast Systems Helios Fire spectrophotometer. The system is equipped with a 7 W, 1028 nm laser, where the fundamental frequency is doubled to provide 524 nm excitation with pulse widths of 250 fs. A white light continuum of similar pulse width is used as a probe pulse to monitor the transient absorption signal. Absorption measurements are

recorded on a fs-to-ns timescale. Transient absorption 3D plots were processed using Surface Explorer and kinetics was analyzed with Origin Pro.

ASSOCIATED CONTENT

Supporting Information

The Supporting Information is available free of charge on the ACS Publications website at DOI:

Structural reorganizations in and of **1** and their potential impact on singlet fission efficiency; comparison of the frontier orbitals and transition dipole moments of **1** and pentacene; more details of the three components of the transient absorption spectrum of **1**; calculation results and discussions of the other six $(BN)_2$-pyrenes that do not satisfy $E() > 2E()$; active orbitals and their occupation numbers of the ground state of **1**; coordinates of all investigated structures.

AUTHOR INFORMATION

Corresponding Author

* toby.zeng@carleton.ca

* kevin.stamplecoskie@queensu.ca

Notes

The authors declare no competing financial interest.

ACKNOWLEDGEMENTS

We thank Mark Gordon and Michael Schmidt for their continuing development of the GAMESS-US program package. All authors thank the Natural Sciences and Engineering Research Council (NSERC) of Canada (T.Z.: No. RGPIN-2016-06276; S.K.M., D.Y. X.W. and S.W.: No. RGPIN-11993993-2013; K.S.: RGPIN-2016-05070) for funding and T.Z. thanks Carleton University (No. 186853) for start-up grant. We thank Samuel Sanders and Andrew Musser for enlightening discussions.